

Mechanistic Insights into Solvent-Controlled Stepwise and Concerted Cycloadditions of the Propadienyl Cation with Oxoamides: A DFT Study

Vanishree Shankar Naik¹, Nayela Javeed¹, Ganga Periyasamy^{2,*}

Abstract

Oxazoles constitute an important class of heterocycles with widespread applications in medicinal chemistry and materials science, yet the mechanistic features governing their formation via cationic cycloaddition reactions remain incompletely understood. In this work, we present a comprehensive density functional theory (DFT) investigation into the reaction between the propadienyl cation and oxoamides as a model system for oxazole ring formation. Using the CAM-B3LYP/6–31+G(d,p) level of theory, we systematically compare gas-phase reactivity with implicit (PCM) and explicit solvation effects in water, acetonitrile, and dichloromethane. Our results reveal that in the gas phase, the reaction preferentially proceeds through a stepwise ionic mechanism, while a concerted [3+2] cycloaddition pathway is energetically inaccessible without geometric constraints. Inclusion of implicit solvation fundamentally alters the reaction landscape, stabilizing polarized transition states and enabling a viable concerted pathway with solvent-dependent activation barriers. Explicit solvation further lowers the activation energies, particularly in polar solvents, through specific hydrogen-bonding and dipole–dipole interactions that stabilize charge development along the reaction coordinate. Quantitative comparison shows that explicit solvation reduces concerted activation barriers by up to 4 kcal mol⁻¹ relative to implicit models and significantly stabilizes ionic intermediates in stepwise pathways. This study demonstrates that solvent effects are decisive in controlling both the feasibility and mechanism of propadienyl-cation-mediated oxazole formation. The insights gained highlight the importance of incorporating explicit solvation for accurately modeling highly polarized cycloaddition reactions and provide a rational basis for solvent-controlled, regioselective synthesis of oxazole derivatives. These findings offer guidance for experimental design, catalyst selection, and modeling of heterocycle synthesis.

Keywords: Cationic cycloaddition, density functional theory (DFT), explicit solvation modeling, oxazole synthesis, solvent effects

*Author for Correspondence

Ganga Periyasamy
E-mail: Ganga.periyasamy@gmail.com

¹Student, Department of Chemistry, Bangalore University, Bangalore, Karnataka, India.

²Assistant Professor, Department of Chemistry, Bangalore University, Bangalore, Karnataka, India.

Received Date: January 21, 2026

Accepted Date: February 01, 2026

Published Date: February 05, 2026

Citation: Vanishree Shankar Naik, Nayela Javeed, Ganga Periyasamy. Mechanistic Insights into Solvent-Controlled Stepwise and Concerted Cycloadditions of the Propadienyl Cation with Oxoamides: A DFT Study. International Journal of Thermodynamics and Chemical Kinetics. 2026; 12(1): 8–17p.

INTRODUCTION

Oxazoles represent an important class of five-membered heterocycles containing both nitrogen and oxygen atoms [1], and their unique electronic structure makes them central scaffolds in modern organic and medicinal chemistry [2]. The oxazole nucleus is widely distributed in natural products [3], bioactive small molecules [4], and pharmaceutical candidates [5], where its heteroatom arrangement imparts distinct hydrogen-bonding features, dipole moments [6], and aromatic stabilization [7]. These properties contribute to a broad spectrum of biological activities reported for oxazole derivatives, including antibacterial [7], anticancer [8], anti-inflammatory [9], antimalarial [10], antifungal [11], and antioxidant effects [12]. In addition to medicinal

value, oxazole-based systems have also gained significance in materials science, where they serve as functional units in organic conductors, semiconductors [13], optoelectronic devices [14], and fluorescence-based probes owing to their tunable electronic and photophysical characteristics [15].

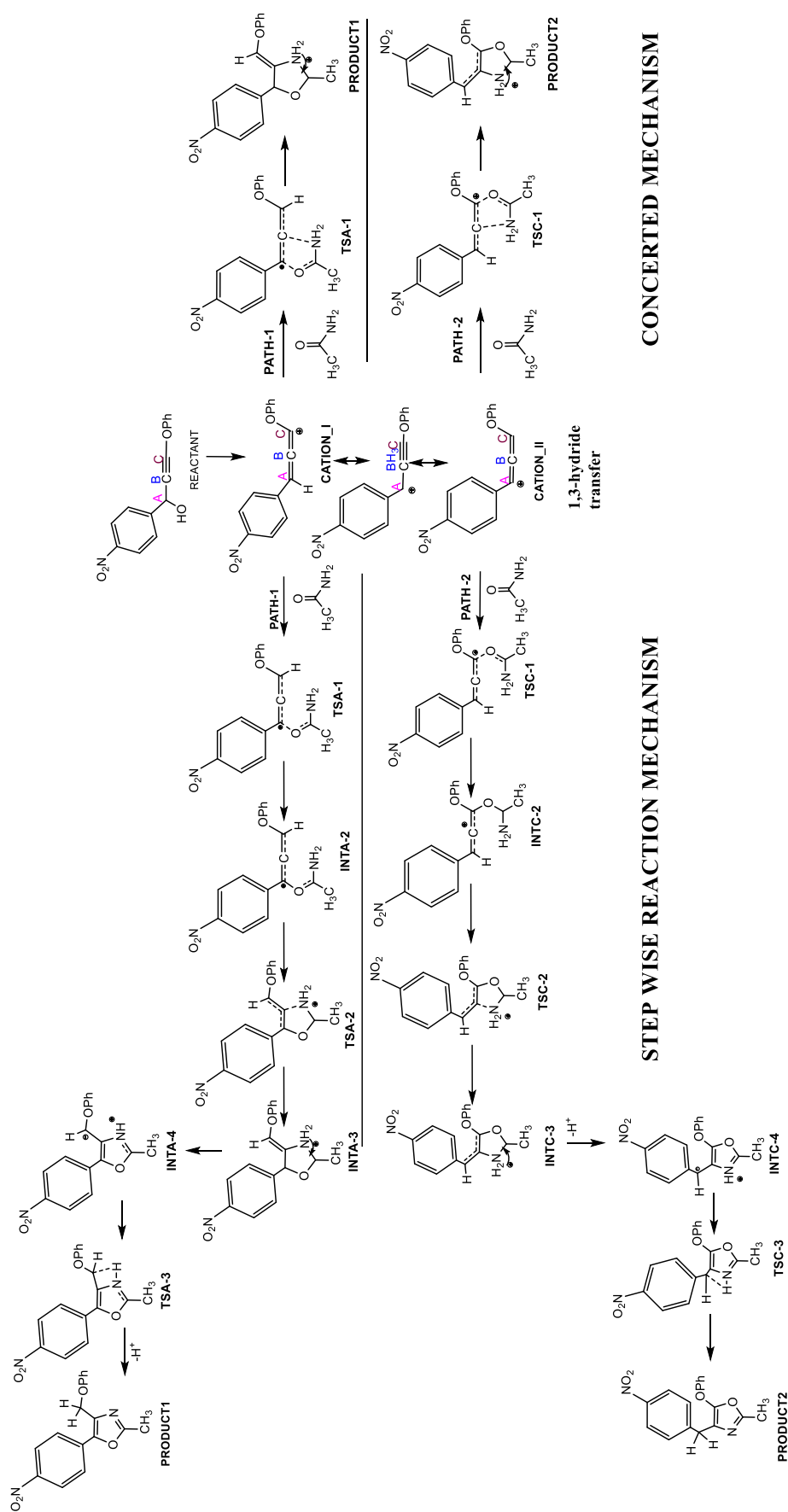
Numerous synthetic strategies have been developed for constructing oxazole rings, among which 1,3-dipolar cycloadditions remain a powerful and widely applied approach [15, 16]. These reactions allow rapid formation of five-membered heterocycles with predictable regioselectivity [17]. Recently, the propadienyl cation (allenyl ion) has emerged as an unconventional yet highly promising 1,3-dipolar component capable of engaging polarized heteroatom-containing dipolarophiles to generate new heterocycles [18]. The strong π -delocalization and high electrophilicity of the propadienyl cation enable efficient interaction with oxygen- and nitrogen-containing functional groups [19], making oxoamide-based systems a particularly attractive target for oxazole synthesis. Despite its growing synthetic utility, the mechanistic understanding of propadienyl-cation-driven cycloadditions leading to oxazole frameworks remains incomplete. In particular, the influence of solvent polarity, dielectric stabilization [19], and specific solute–solvent interactions on the competition between stepwise ionic routes and concerted cycloaddition [19] pathways is not yet well established. Given the highly charged and reactive nature of the propadienyl cation, these factors are expected to play a decisive role in determining both reaction feasibility and regioselectivity [20].

The present work addresses this gap by performing a detailed DFT investigation on the reaction between the propadienyl cation and oxoamides as precursors for oxazole ring formation. By comparing gas-phase results with implicit solvation and explicit first-shell solvation models [21] (acetonitrile, dichloromethane, and water), we aim to elucidate how solvent environments shape the potential energy surface and govern the preferred reaction pathway. This mechanistic insight provides a foundation for designing solvent-controlled, regioselective strategies for constructing oxazole derivatives using cumulene-based cationic synthons [21].

COMPUTATIONAL DETAILS

All quantum-chemical calculations were performed using Density Functional Theory (DFT) as implemented in the Gaussian 09 package [22]. Geometry optimizations and frequency calculations for all reactants, intermediates, transition states, and products were carried out using the long-range-corrected CAM-B3LYP functional with the 6–31+G(d,p) basis set [23], chosen for its reliability in describing charge-separated systems, cumulenes, and transition states involving significant polarization. Frequency analyses were used to confirm the nature of all stationary points, ensuring that minima displayed no imaginary frequencies and transition states exhibited exactly one. Intrinsic Reaction Coordinate (IRC) calculations were subsequently performed to verify the connectivity of each transition state to its corresponding reactant and product minima. To assess solvent effects, both implicit and explicit solvation approaches were employed. Implicit solvation was included using the SCRF/PCM [24] continuum model in three solvents – acetonitrile, dichloromethane, and water. The explicit solvation [25] was explored by incorporating three/four explicit solvent molecules around the propadienyl cation and critical transition states, followed by reoptimization within and without the continuum. Electronic-structure analyses, including HOMO–LUMO energies, were obtained from the optimized structures to evaluate the electrophilicity of the propadienyl cation and the nucleophilic character of the oxoamide, aiding in the interpretation of regioselectivity and the competition between concerted and stepwise pathways. Tight SCF convergence criteria and ultrafine integration grids were applied throughout to ensure numerical accuracy.

Below is a comprehensive, publication-ready Results and Discussion section tailored to your study: reaction of the propadienyl cation with oxoamide, comparison of concerted vs. stepwise pathways, and influence of implicit and explicit solvation (ACN, DCM, water) using CAM-B3LYP/6–31+G(d,p).



RESULTS AND DISCUSSION

The reaction between the propadienyl cation and oxoamide was examined to understand the mechanistic competition between a concerted [3+2] cycloaddition leading directly to the oxazole ring and a stepwise pathway involving discrete ionic intermediates. The optimized structures and computed Gibbs free energies reveal that in the gas phase, the highly electrophilic propadienyl cation readily forms a weakly bound pre-reactive complex with the carbonyl oxygen of the oxoamide. This interaction is dominated by charge–dipole stabilization, which orients the dipolarophile in a manner favoring nucleophilic attack on the cumulene center. Our earlier studies on Frontier molecular orbital (FMO) analysis, show that the low-lying LUMO of the propadienyl cation (localized over the central C=C=C unit) interacts strongly with the oxoamide HOMO, supporting a polar, asynchronous transition state even in the gas phase.

Gas-Phase Mechanistic Landscape

In our earlier work [18], we demonstrated that the [3+2] cycloaddition can proceed either through a highly asynchronous concerted pathway or via a more favorable stepwise mechanism involving well-defined intermediates and transition states. Both pathways originate from the same reactant but differ fundamentally in the sequence and coupling of the elementary steps involved.

In the stepwise mechanism, the reaction is initiated by protonation or electrophilic activation, leading to the formation of a stabilized cationic intermediate (INTA/INTC). This species undergoes structural reorganization through a distinct transition state (TSA/TSC), followed by successive bond-forming and bond-breaking events to yield additional intermediates (INTA-2/INTC-2, INTA-3/INTC-3 and INTA-4/INTC-4). Each step is associated with a discrete energy barrier, enabling effective charge delocalization and allowing substituent effects to play a decisive role in stabilizing the intermediates. Variations in substituent orientation and migration give rise to two competing pathways (Path 1 and Path 2), ultimately leading to regioselective formation of PRODUCT 1 or PRODUCT 2.

In contrast, the concerted mechanism proceeds through a single, highly organized transition state in which bond formation, bond cleavage, and proton transfer occur simultaneously, without the involvement of isolable intermediates. This pathway features a cyclic or tightly associated transition structure that minimizes charge separation. Consistent with our previous findings, gas-phase calculations in the present study indicate that the concerted transition state cannot be located without imposing geometric constraints, whereas the stepwise pathway remains energetically viable for all substituents examined, including the strongly electron-withdrawing NO₂ group. Building on this mechanistic framework, the current study further investigates the role of implicit and explicit solvation in modulating the reaction energy landscape and regioselectivity.

Implicit Solvation Effects (PCM Model)

The implicit solvation model plays a crucial role in stabilizing the reaction pathway, particularly the concerted transition state (TS), which is not feasible without constraints in the gas phase. In polar (water), moderately polar (acetonitrile, ACN), and weakly polar (dichloromethane, DCM) solvents, the dielectric medium effectively screens charge separation and stabilizes the developing polarization at the TS. As shown in the concerted energy profile in Figure 1a, all solvents display a single, well-defined TS connecting reactants directly to products, indicating a synchronous bond-forming and bond-breaking process without the formation of discrete intermediates. This stabilization arises from solvent-induced electrostatic screening, which lowers the energetic penalty associated with simultaneous electronic reorganization. In contrast, such a concerted TS cannot be located in the gas phase due to the absence of dielectric stabilization, leading instead to a stepwise mechanism.

For the stepwise pathway in Figure 1b, the energy values clearly reflect solvent-dependent stabilization effects. In the gas phase, Path-I (P1) shows higher activation barriers (17.01 kcal mol⁻¹ and 15.22 kcal mol⁻¹) and relatively poor product stabilization (−1.98 kcal mol⁻¹), indicating kinetically and thermodynamically less favorable progress due to unshielded charge buildup. Path-II (P2), although

exhibiting a slightly lower initial barrier (16.50 kcal mol⁻¹), encounters a significantly higher subsequent barrier (19.60 kcal mol⁻¹), reflecting substantial electronic and structural reorganization that is energetically costly in the absence of solvation. However, P2 ultimately leads to a more stabilized product (-4.20 kcal mol⁻¹), suggesting thermodynamic preference but with kinetic penalty.

Under implicit solvation, these barriers are significantly reduced and smoothed. Water provides the strongest stabilization, owing to its high dielectric constant, followed by ACN, which efficiently stabilizes polar TSs without hydrogen bonding, and DCM, which offers weaker but still noticeable stabilization. As a result, both P1 and P2 exhibit lowered activation energies and deeper intermediate stabilization compared to the gas phase. Importantly, this solvent stabilization enables the concerted pathway to become viable, as reflected in the single-hump energy profiles in the Figure 1, with the lowest TS energies observed in water, followed by ACN and DCM.

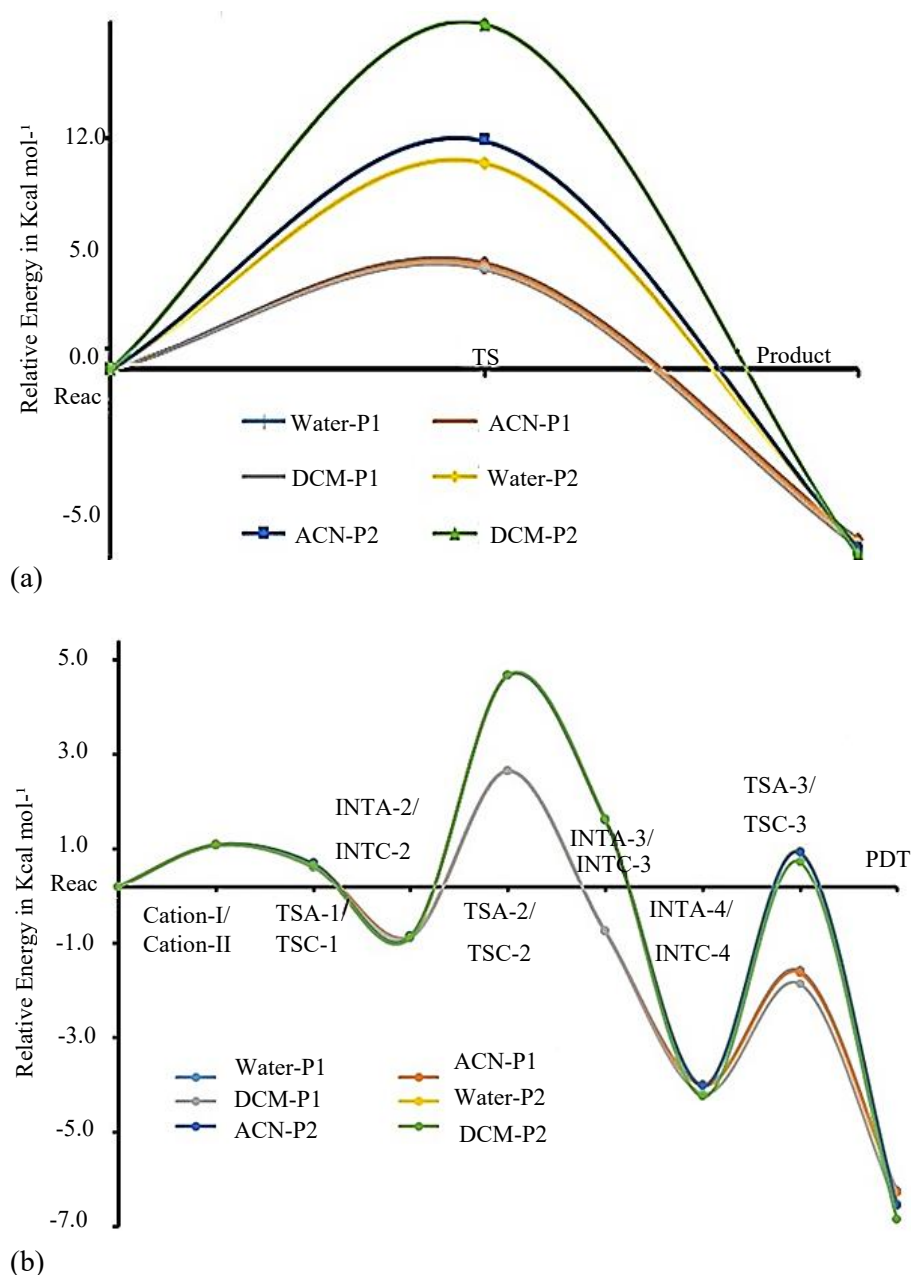


Figure 1. Relative energy profiles with respect to the reactants obtained using the PCM model illustrating (a) the concerted reaction pathway and (b) the stepwise reaction pathway.

The results mentioned above demonstrate that implicit solvation not only lowers activation barriers for the stepwise mechanism but also fundamentally alters the reaction landscape by stabilizing a concerted TS, which is inaccessible in the gas phase. This highlights the decisive role of solvent polarity in governing the reaction mechanism, shifting the system from a stepwise pathway in the gas phase to a concerted pathway under solvated conditions.

Explicit Solvation Effects

The optimized geometries clearly illustrate the structural evolution of the reaction along both the stepwise and concerted pathways. For the stepwise mechanism, the transition states (Reactant, Cation-I, TSA-1, TSA-2, and TSA-3 for Path-1; Reactant, Cation-2, TSC-1, TSC-2, and TSC-4 for Path-2) are characterized by partially formed and elongated bonds, confirming asynchronous bond reorganization (Figure 2). In TSA-1/TSC-1, the initial bond activation is evident from the elongated reacting bond distances, indicating the onset of nucleophilic attack and charge development. The corresponding intermediates (INTA-2, INTA-3, INTA-4 and INTC-1, INTC-3, INTC-4) exhibit stabilized geometries with fully formed or significantly shortened bonds, reflecting charge delocalization and structural relaxation after each elementary step. The gradual shortening and lengthening of specific bonds across successive TS–INT pairs clearly support a stepwise reaction sequence with distinct intermediates.

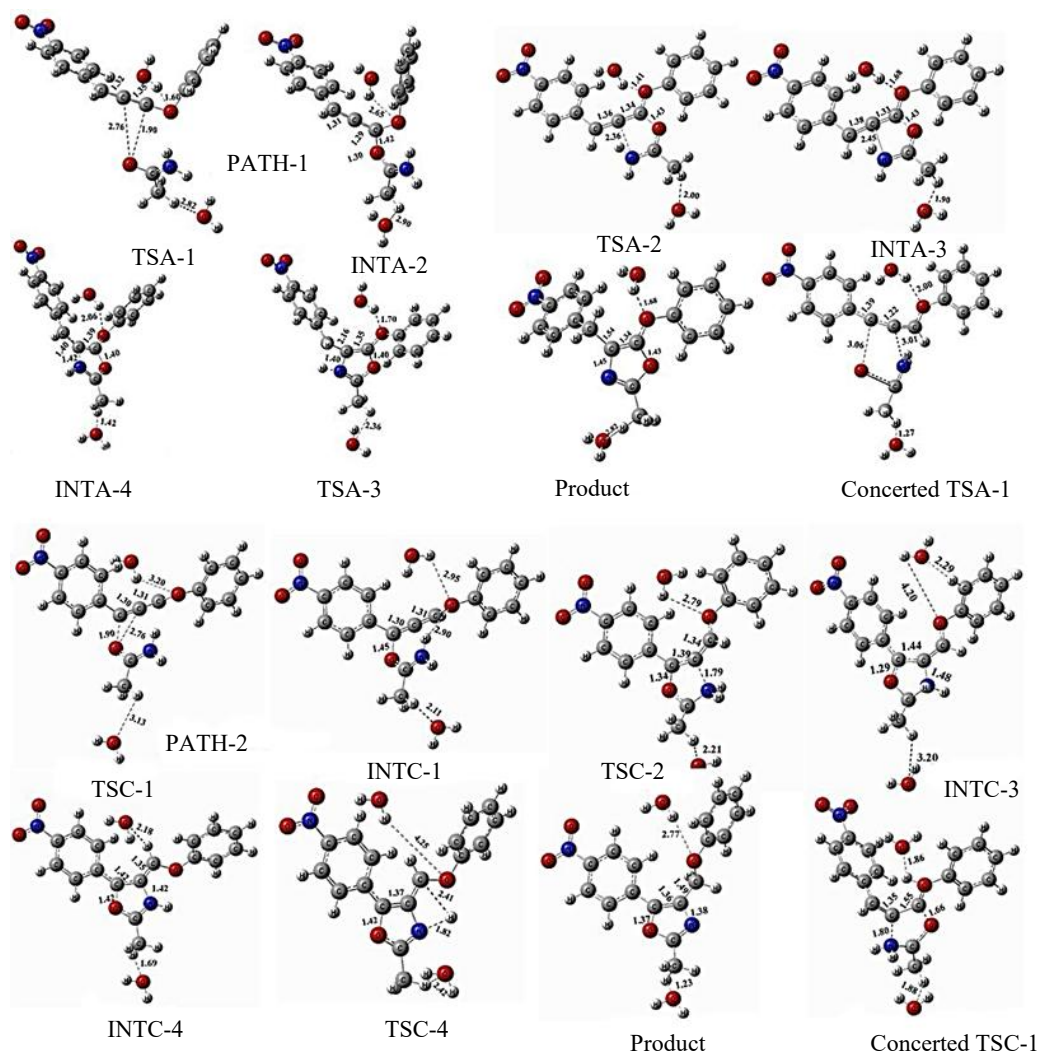


Figure 2. Optimized geometries of key stationary points along the stepwise and concerted reaction pathways Path-I and Path-2, including transition states (TS), intermediates (INT), and products, highlighting the evolution of critical bond distances in Å during bond formation and cleavage.

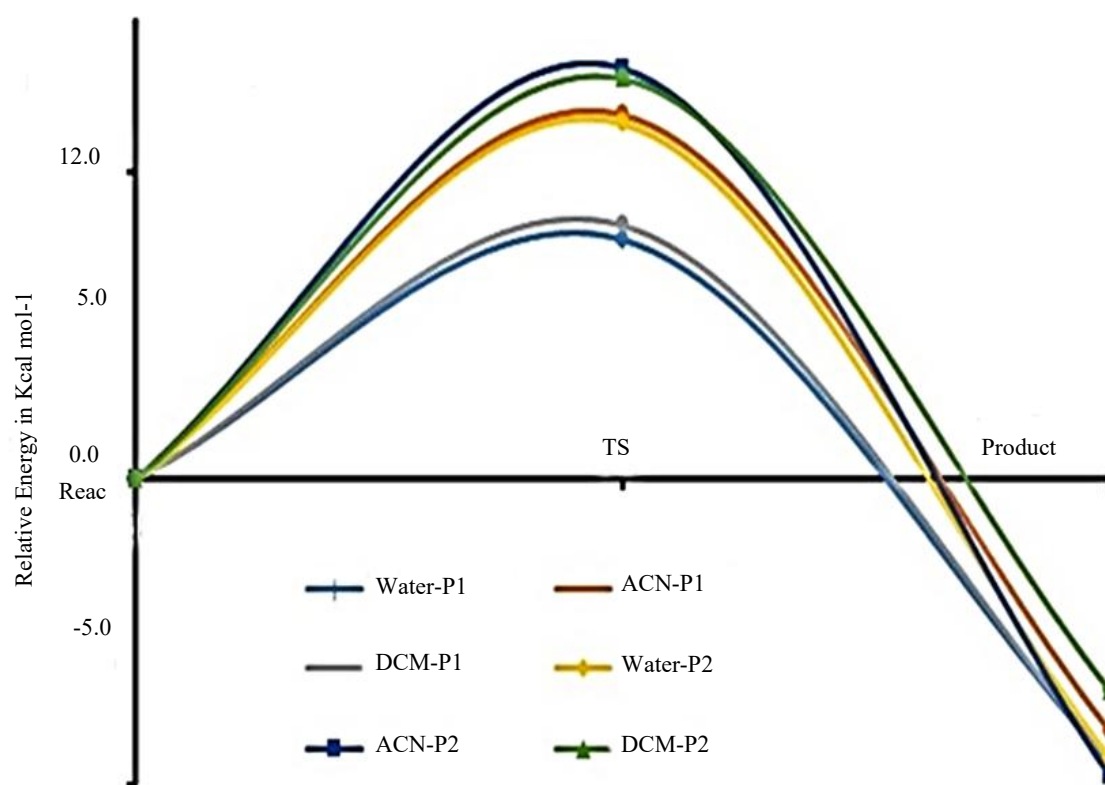
In contrast, the concerted transition states (Concerted TSA-1 and Concerted TSC-1) show simultaneous bond formation and bond cleavage within a single optimized structure. These geometries display nearly synchronous changes in the key reacting bond distances, with both bonds partially formed/cleaved at the TS, and without the presence of any stable intermediate. This structural feature is consistent with a concerted mechanism and correlates well with the single-hump energy profile observed under implicit solvation.

The product geometries obtained from both mechanisms are fully relaxed and show well-defined bond lengths corresponding to the final stable configuration, confirming that both pathways converge to the same thermodynamic product. The optimized geometries provide strong structural evidence that the reaction proceeds via a stepwise mechanism in the absence of sufficient stabilization, while implicit solvation enables a concerted pathway by stabilizing the highly polarized transition state.

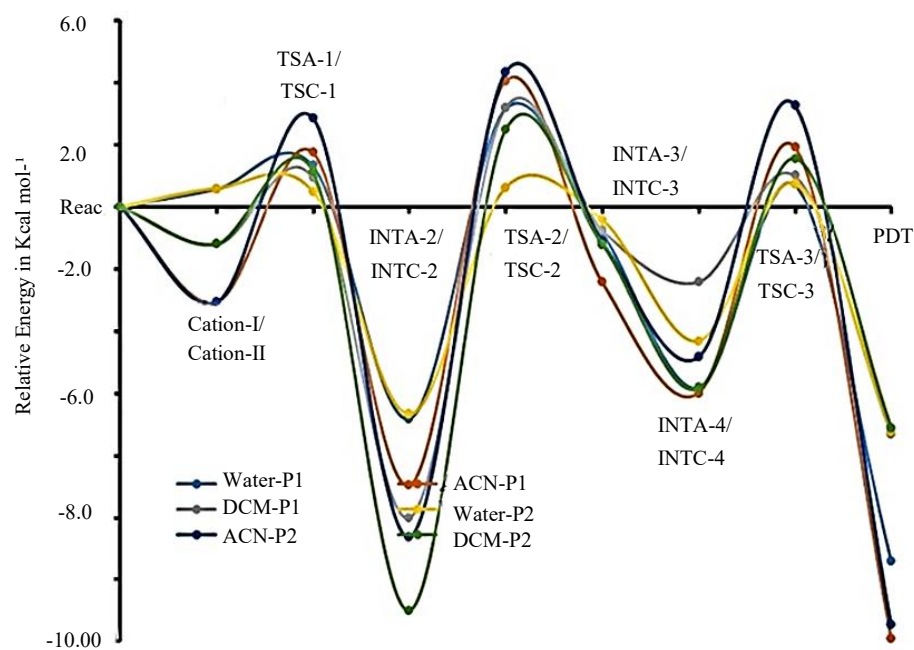
Explicit Solvation: Energy Barriers and Trends

Under explicit solvation, the concerted pathway exhibits significantly reduced activation barriers compared to the stepwise route. From Figure 3 (a), the concerted activation barriers are approximately 4–5 kcal mol⁻¹ in water, ~4 kcal mol⁻¹ in ACN, and ~13–14 kcal mol⁻¹ in DCM (P2). The markedly lower barriers in water and ACN arise from direct hydrogen bonding (water) and strong dipole–dipole stabilization (ACN) of the polarized concerted transition state. DCM, lacking strong specific interactions, shows the highest barrier.

For the stepwise mechanism under explicit solvation (Figure 3b), the first transition state (TSA-1/TSC-1) lies close to the reactant energy (≈ 0 to 1 kcal mol⁻¹), while the second transition state (TSA-2/TSC-2) represents the rate-determining step, with barriers of approximately 4.5–5.0 kcal mol⁻¹ in DCM, ~2.5–3.0 kcal mol⁻¹ in ACN, and ~1.5–2.0 kcal mol⁻¹ in water. Deep stabilization of intermediates (down to -4 to -6 kcal mol⁻¹) is observed, particularly in water, reflecting strong explicit solvation of charged species.



(a)



(b)

Figure 3. Relative energy profiles with respect to the reactants obtained using the PCM model illustrating (a) the concerted reaction pathway and (b) the stepwise reaction pathway.

Comparison Between Explicit and Implicit Solvation

The explicit solvation yields lower concerted activation barriers when compared to implicit solvation model, typically in the range of 7–8 kcal mol⁻¹ (water-P1), ~12 kcal mol⁻¹ (ACN-P2), and ~14–15 kcal mol⁻¹ (DCM-P2). Although PCM effectively captures dielectric screening, it lacks specific solute–solvent interactions, resulting in less stabilization of the concerted transition state compared to explicit solvation.

For the stepwise pathway, implicit solvation produces shallower intermediates (≈ -2 to -4 kcal mol⁻¹) and higher subsequent barriers (TSA-2/TSC-2 ≈ 2 –4 kcal mol⁻¹), reflecting uniform dielectric stabilization without accounting for solvent shell reorganization. Compared to this, explicit solvation lowers intermediate energies by ~1–3 kcal mol⁻¹ but does not proportionally reduce all transition-state barriers due to the energetic cost of solvent reorientation during bond reorganization.

Mechanistic Explanation of the Differences

The lower barriers under explicit solvation arise from localized stabilization of developing charges through hydrogen bonding and directional electrostatics, which are absent in PCM. This effect is most pronounced for the concerted transition state, where simultaneous bond formation and cleavage generate strong polarization. In the stepwise pathway, explicit solvation preferentially stabilizes ionic intermediates, deepening energy wells and sometimes increasing the relative height of subsequent barriers due to solvent reorganization penalties.

Quantitatively, explicit solvation lowers concerted activation barriers by ~2–4 kcal mol⁻¹ relative to implicit solvation in polar solvents, while enhancing intermediate stabilization by ~1–3 kcal mol⁻¹ in the stepwise mechanism. As a result, explicit solvation strengthens the kinetic preference for the concerted pathway, particularly in water, and provides a more realistic depiction of solvent-controlled reactivity than the implicit model.

CONCLUSION

In this work, a detailed DFT analysis has been carried out to elucidate the mechanistic pathways governing oxazole formation from the reaction of the propadienyl cation with oxoamides. The

combined examination of gas-phase, implicit solvation, and explicit solvation models provides a comprehensive understanding of how solvent environments modulate the reaction energy landscape. In the gas phase, the reaction proceeds predominantly through a stepwise ionic mechanism, as the highly polarized concerted transition state cannot be stabilized in the absence of dielectric screening. The stepwise pathway involves well-defined intermediates and multiple transition states, reflecting significant charge separation and asynchronous bond reorganization. Inclusion of implicit solvation using the PCM model markedly stabilizes charge-separated species and lowers activation barriers for both stepwise and concerted pathways. Notably, implicit solvation enables the emergence of a viable concerted cycloaddition mechanism, which is entirely inaccessible in the gas phase. Among the solvents studied, water provides the greatest stabilization, followed by acetonitrile and dichloromethane, consistent with their dielectric properties. Explicit solvation further refines this mechanistic picture by capturing specific solute–solvent interactions that are absent in continuum models. Hydrogen bonding in water and strong dipole–dipole interactions in acetonitrile substantially lower the concerted activation barriers and deepen the stabilization of ionic intermediates in the stepwise pathway. Quantitatively, explicit solvation reduces concerted activation barriers by approximately 2–4 kcal mol⁻¹ relative to implicit solvation and enhances intermediate stabilization by 1–3 kcal mol⁻¹, underscoring the importance of first-shell solvent effects. The results mentioned above demonstrate that solvent polarity and specific solvation play a decisive role in dictating whether the reaction proceeds via a stepwise or concerted pathway. The results highlight the necessity of explicit solvation models for accurately describing highly polarized cycloaddition reactions involving cationic cumulenes. These mechanistic insights provide a valuable framework for designing solvent-controlled and regioselective synthetic strategies for oxazole derivatives and related heterocyclic systems.

Acknowledgments

G. P. and V. S. is grateful to the UGC–BSR (2013–21FRP), and the Vision Group on Science and Technologies (VGST–KFIST–L2/GRD–1021/118/2022–23/94), Bangalore University for funding.

REFERENCES

1. Kadu VD. Recent advances for synthesis of oxazole heterocycles via C–H/C–N bond functionalization of benzylamines. *ChemistrySelect*. 2022;7(22).
2. Joshi S, Mehra M, Singh R, Kakar S. Review on chemistry of oxazole derivatives: Current to future therapeutic prospective. *Egypt J Basic Appl Sci*. 2023;10(1):218–39.
3. Yeh VSC. Recent advances in the total syntheses of oxazole-containing natural products. *Tetrahedron*. 2004;60(52):11995–2042.
4. Kakkar S, Narasimhan B. A comprehensive review on biological activities of oxazole derivatives. *BMC Chem*. 2019;13(3):1–24.
5. Turchi IJ. E : Jxc : R. *Ind Eng Chem Prod Res Dev*. 1981;20(1):32–76.
6. Chopra N, Kaur D, Chopra G. Hydrogen bonded complexes of oxazole family: Electronic structure, stability, and reactivity aspects. *Struct Chem*. 2018;29(1):341–57.
7. Shaffer AA, Wierschke SG. Comparison of computational methods applied to oxazole, thiazole, and other heterocyclic compounds. *J Comput Chem*. 1993;14(1):75–88.
8. Pearce S. The importance of heterocyclic compounds in anti-cancer drug design. *Drug Discov World*. 2017;18(2):66–70.
9. Sharma S, Kumar D, Singh G, Monga V, Kumar B. Recent advancements in the development of heterocyclic anti-inflammatory agents. *Eur J Med Chem*. 2020;200:112438.
10. Chugh A, Kumar A, Verma A, Kumar S, Kumar P. A review of antimalarial activity of two or three nitrogen atoms containing heterocyclic compounds. *Med Chem Res*. 2020;29(10):1723–50.
11. Kathiravan MK, Salake AB, Chothe AS, Dudhe PB, Watode RP, Mukta MS, et al. The biology and chemistry of antifungal agents: A review. *Bioorg Med Chem*. 2012;20(19):5678–98.
12. Saat K, Moniczewski A, Librowski T. Mini-reviews in medicinal chemistry. *Mini Rev Med Chem*. 2013;13:335–52.
13. Editorial G. Special issue: Sulfur-nitrogen heterocycles. *Chem Rev*. 2005;318–20.

14. Ramkumar V, Kannan P. Novel heterocyclic based blue and green emissive materials for optoelectronics. *Opt Mater (Amst)*. 2015;46:314–23.
15. Suresha S, Shilpa GM, Mohsen Q, Alsuhaibani AM, Pandurangappa C, Prabhala P, et al. A comprehensive study on the photophysical properties and solvatochromic behavior of fluorescent oxazole for deep blue OLED applications. *J Fluoresc*. 2025.
16. Meyer AG, Ryan JH. 1,3-Dipolar cycloaddition reactions of azomethine ylides with carbonyl dipolarophiles yielding oxazolidine derivatives. *Molecules*. 2016;21(8).
17. Ghomri A, Mekelleche SM. Reactivity and regioselectivity of five-membered heterocycles in electrophilic aromatic substitution: A theoretical investigation. *J Mol Struct THEOCHEM*. 2010;941(1–3):36–40.
18. Naik VS, Periyasamy G. Exploring regioselectivity in 1,3-dipolar cycloaddition of thioamides, selenoamides, and amides with propadienyl cation derivatives using density functional theory. *J Phys Org Chem*. 2024;37(10):1–11.
19. Wipf P, Aoyama Y, Benedum TE. A practical method for oxazole synthesis by cycloisomerization of propargyl amides. *Org Lett*. 2004;6(20):3593–5.
20. Sigmund LM, Assante M, Johansson MJ, Norrby PO, Jorner K, Kabeshov M. Computational tools for the prediction of site- and regioselectivity of organic reactions. *Chem Sci*. 2025;16(13):5383–412.
21. Ramirez R, Borgis D. Density functional theory of solvation and its relation to implicit solvent models. *J Phys Chem B*. 2005;109(14):6754–63.
22. Frisch MJ, Trucks GW, Schlegel HB, Scuseria GE, Robb MA, Cheeseman JR, et al. *Gaussian*. Gaussian Inc. 2009.
23. Yanai T, Tew DP, Handy NC. A new hybrid exchange-correlation functional using the Coulomb-attenuating method (CAM-B3LYP). *Chem Phys Lett*. 2004;393(1–3):51–7.
24. Houjou H, Sakurai M, Inoue Y. Theoretical evaluation of medium effects on absorption maxima of molecular solutes. I. Formulation of a new method based on the self-consistent reaction field theory. *J Chem Phys*. 1997;107(15):5652–60.
25. Cossi M, Barone V, Cammi R, Tomasi J, Mennucci B, et al. Recent advances in the description of solvent effects with the polarizable continuum model. *Adv Quantum Chem*. 1999;32:227–61.